



# Sodium selenite attenuates lung adenocarcinoma progression by repressing SOX2-mediated stemness

Weiwei Chen<sup>1</sup> · Jiajia An<sup>1</sup> · Jiwei Guo<sup>1</sup> · Yan Wu<sup>1</sup> · Lijuan Yang<sup>1</sup> · Juanjuan Dai<sup>1</sup> · Kaikai Gong<sup>1</sup> · Shuang Miao<sup>1</sup> · Sichuan Xi<sup>1</sup> · Jing Du<sup>1</sup>

Received: 27 December 2017 / Accepted: 11 March 2018 / Published online: 15 March 2018  
© Springer-Verlag GmbH Germany, part of Springer Nature 2018

## Abstract

**Purpose** Sodium selenite (SS) has been widely reported to induce apoptosis in various cancer cell types. However, the underlying molecular mechanisms governing SS-mediated repression of lung cancer stem cells remain largely undefined.

**Methods** In vitro assays of cell proliferation, clonal formation, apoptosis, migration and cancer stemness cell sphere formation were performed to examine the inhibitory effects of SS on lung adenocarcinoma (LAD) cells with or without the overexpression of SRY-related high-mobility-group box 2 (SOX2).

**Results** SS significantly inhibited cell growth and induced apoptosis in LAD cells in a dose-dependent manner with marginal effects on normal epithelial cell HBEC. SS dramatically repressed expression of SOX2 and its upstream regulator GLI1 and strongly decreased stemness sphere formation in LAD cells at 10  $\mu$ M. Forced expression of SOX2 significantly buffered anti-cancer effects of SS.

**Conclusions** Our results demonstrate that SS attenuates lung adenocarcinoma progression by repressing SOX2 and its upstream regulator GLI1, which suggests that SS may be a potential therapeutic drug candidate for lung cancer patients.

**Keywords** Lung adenocarcinoma (LAD) · Sodium selenite (SS) · SOX2 · Hedgehog · CSCs

## Introduction

As a leading cause of cancer-related mortality in the world, non-small cell lung cancer (NSCLC) consists of several pathological subtypes, among which lung adenocarcinoma (LAD) accounts for 50% of all NSCLC cases and lung squamous cell carcinoma (LSC) claims around 40% of all NSCLC patients [1, 2]. Conventional chemotherapy agents usually produce severe unbearable side effects in patients. Although current available auxiliary therapies with EGFR and ALK tyrosine kinase inhibitors have increased survival ability and life qualities of lung cancer patients over the last

decade, those treatments are not sufficient to prevent patients with LAD from transient relapses with drug resistance development and tumor metastasis [3, 4]. Accumulating evidence has suggested that cancer stemness cells (CSCs) were involved in drug resistance and tumor metastasis due to their unlimited proliferative capability and multiple differentiation potential [5]. Therefore, CSC-specific inhibitory drugs with tolerable side effects may gain more potential therapeutic benefit in clinic.

SOX2, one of the SOX family members, plays a pivotal role in cancer stem cell self-renewal and multiple differentiation potential. As a stem cell transcription factor, SOX2 has been reported to be highly expressed in NSCLC stem cells and closely related to the initiation and maintenance CSCs [6]. In the meantime, Glioma-associated oncogene 1 (GLI1), a dominant component of Hedgehog cascade, acts as a positive upstream regulator via specific enrichments in the promoter region of SOX2 to mediate stemness cell proliferation and drug resistance [7]. The sonic hedgehog (SHH) pathway not only physiologically regulates cell proliferation and differentiation during embryonic development but also plays a significant role in the tumorigenicity

---

Weiwei Chen and Jiajia An equally contributed.

✉ Sichuan Xi  
xh\_xi@yahoo.com

✉ Jing Du  
jing\_pumc@hotmail.com

<sup>1</sup> Cancer Research Institute, Binzhou Medical University Hospital, No. 661 Huanghe Street, Binzhou 256600, Shandong, People's Republic of China

of CSCs [8]. Key components of the SHH pathway such as Patched receptor (PTCH), Smoothed protein (SMO) and GLI1 were reported to be actively expressed in various cancer types including lung cancer [9, 10]. We and other groups have reported that specific inhibition of SMO or GLI1 could sensitize lung cancer cells to both standard and targeted therapy [11–13].

Selenium, an essential trace element in human health, has recently been found to play a beneficial role in cancer therapy [14, 15]. Selenium has been identified as a chemotherapeutic candidate via inducing cancer cell apoptosis with minimal side effects at a proper concentration range [16, 17]. Extensive studies have shown that selenium and its derivative sodium selenite (SS) could induce apoptosis in various cancer cells including prostate, colon, breast, cervical and lung cancer cells at tolerable concentrations [18–24]. In prostate cancer, SS could activate cancer repressor gene PTEN and sensitize hormone-refractory prostate cancer cells to radiotherapy in vivo [25, 26]. In addition to directly targeting neoplastic cells, SS was found to alleviate chemo- and radiotherapy-related lymphedema and other complications in patients [27]. Whether SS could repress lung CSCs and how the underlying molecular mechanisms governs this process remain to be further investigated.

In the present study, we explored effects of SS on LAD parental cell growth and stemness spheroid formation. Herein, we report that SS attenuates lung adenocarcinoma progression by repressing SOX2 and its upstream regulator GLI1, which suggests that SS may be a potential therapeutic drug candidate for lung cancer patients.

## Materials and methods

### Cell culture and reagents

The LAD cell lines A549 and H1299 were obtained from American Type Culture Collection (ATCC). The LAD cell line PC9 and normal human epithelial bronchial cell HBEC (immortalized with CDK4 and hTERT) were obtained from National Cancer Institute (USA). All three LAD cell lines were maintained in DMEM medium supplemented with 10% fetal bovine serum (Hyclone, USA), 100 units/ml penicillin, and 100 µg/ml streptomycin. HBEC was cultured in DMEM medium supplemented with 20% fetal bovine serum, 5 ng/ml EGF (Peprotech, USA), 100 units/ml penicillin, and 100 µg/ml streptomycin. All cell lines were incubated at 37 °C with 5% CO<sub>2</sub>. Sodium selenite (SS) was purchased from Sigma and dissolved in PBS to 20 mM for storage. Concentrations of SS and durations of incubation were illustrated specifically in each experiment.

### Cell proliferation assay

Cells were automatically counted and seeded at a density of 3000 cells per well into 96-well plate one day before drug treatment. CCK8 (Dojindo, Japan) test was performed 24, 48 and 72 h after various concentrations (0, 5, 10, 20, 40 and 80 µM) of drug incubation according to manufacturer's guide. The absorption and reference wavelengths were measured separately at 450 and 630 nm. Relative proliferation =  $(OD_{450} - OD_{630})_{\text{Sample}} / (OD_{450} - OD_{630})_{\text{Control}}$ .

### Clonal formation assay

Cells were counted and seeded into 12-well plate with 500 cells per well 1 day before drug incubation. Cells were treated with indicated concentrations (0, 5, 10 and 20 µM) of SS for 48 h and then cultured in drug-free medium for another 10 days. Cell clones were fixed with freshly prepared 4% paraformaldehyde and stained with crystal violet (Sangon, China) before optical imaging. Experiments were carried out in triplicates and densitometry analysis was performed with ImageJ software.

### Apoptosis analysis

A549 and H1299 cells treated with various concentrations (0, 5, 10, 20 and 40 µM) of SS for 24 h were collected, washed with ice cold PBS and stained with Annexin V/PI mixture at 4 °C for 30 min according to the manufacturer's instructions (Vazyme, China). After full resuspension, fluorescent signals were measured with CFlow Plus package from Accuri C6. To form four quadrant dot plot, x- and y-axis were set up as FL1 and FL2 channel separately. Dots in left lower quadrant represented viable cells. Dots in right lower and upper quadrants indicated early apoptotic and terminal apoptotic cells, respectively.

### Wound healing assay

Wound healing assay was performed and analyzed as described before [11]. A549 and H1299 cells were seeded into 12-well plate at 10<sup>5</sup> cells per well 1 day before treatment. On the second day, cells were scraped with a 200 µl tip followed by incubation with serum free medium containing 0, 5, 10 and 20 µM SS for 24 or 48 h. Photomicrographs were taken before and after treatment. Relative distances which were calculated by subtracting wound

width before treatment with wound width after treatment were quantified with ImageJ software.

### Transwell migration assay

The transwell migration assay was performed in a 24-well chamber (Corning, USA) according to manufacturer's instructions. The upper and lower chambers were filled with 2000 cells resuspended in DMEM medium free of FBS and normal complete DMEM medium containing 10% FBS, respectively. Cells were allowed to migrate for 72 h before the membrane was fixed and then stained with crystal violet. Cells migrated to the lower side of the membrane were observed under microscope.

### Sphere formation assay

Cells were plated into ultra-low-attachment 12-well plate (Corning, USA) at a density of 1000 cells per well and cultured in serum-free DMEM medium supplemented with 20 ng/ml EGF, 20 ng/ml FGF (Peprotech, USA) and 2% B27 (Gibco, USA). To analyze the inhibitory function of SS on lung CSCs, A549 and H1299 sphere-forming cells were treated with 10  $\mu$ M SS and PBS in parallel as control at the beginning of spheroid culture. Medium was half refreshed every 3 days without new drug addition. Cell spheroids were observed and photographed by an inverted microscope (Olympus, Japan) after 2 weeks.

### Reverse-transcriptase PCR (RT-PCR)

RNA was extracted with Trizol (TransGen Biotech, China) according to the manual's instruction. The purified RNA was reversely transcribed into cDNA with RevertAid First Strand cDNA Synthesis Kit (Fermentas, USA) according to manufacturer's instructions. Polymerase chain reactions were performed with 2 $\times$  Taq Master Mix (Vazyme, China). Primers against SOX2 were GGGAAATGGGAGGGGTGC AAAAGA (Forward) and TTGCGTGAGTGTGGATGG GATTGG (Reverse). Primers for SMO, GLI1 and PTCH were used as published [11].

### Immunoblot

Immunoblot was performed as described before [28]. Cells were collected and lysed with buffer containing protease inhibitors. Total cell protein was separated on sodium dodecyl sulfate-polyacrylamide gels (SDS-PAGE) and transferred to polyvinylidene difluoride (PVDF) membranes (Millipore, USA) by electroblotting. Membranes were incubated with the respective primary antibody (1:1000 dilution) at 4 °C overnight followed by secondary antibodies (1:2000 dilution) incubation. Enhanced chemiluminescence signals

(ECL, Amersham) were detected using the Image Lab software. Antibody against SOX2 was purchased from Abcam (USA). Antibodies used for detecting PTCH, SMO and GLI1 were described before [11].

### Immunofluorescent (if) staining

A549 and H1299 cells were grown on slides in 24-well plate overnight followed with SS treatment for 24 h (Fig. 5d) or not (Figs. 1e, 6b). Cells were fixed in 4% formaldehyde for 30 min, permeabilized with 0.2% Triton X-100 for 10 min and blocked by 2% BSA for 30 min. Coverslips were incubated with SOX2 antibody (Abcam, USA) at 1:200 dilution and subsequently Alexa Fluor 594 (Life Technologies, USA) secondary fluorescence antibody. Hoechst 33342 was used at 2  $\mu$ g/ml for nuclear staining. Images were obtained with Zeiss Axio Imager Z1 Fluorescent Microscope.

### Transfections

A549 and H1299 cells were plated and transiently transfected in 6-well plate using Lipofectamine 2000 (Invitrogen) according to the manufacturer's protocol. pcDNA 3.1 empty vector (pc3.1) and pcDNA 3.1-SOX2 (SOX2) were transfected in parallel. RT-PCR and IF were performed 48 h post transfection to evaluate the expression level of SOX2. For CCK8 and clonal formation assay, cells were seeded into 96 and 12 well plate, respectively, 12 h post transfection for drug treatment as described above.

### Statistical analysis

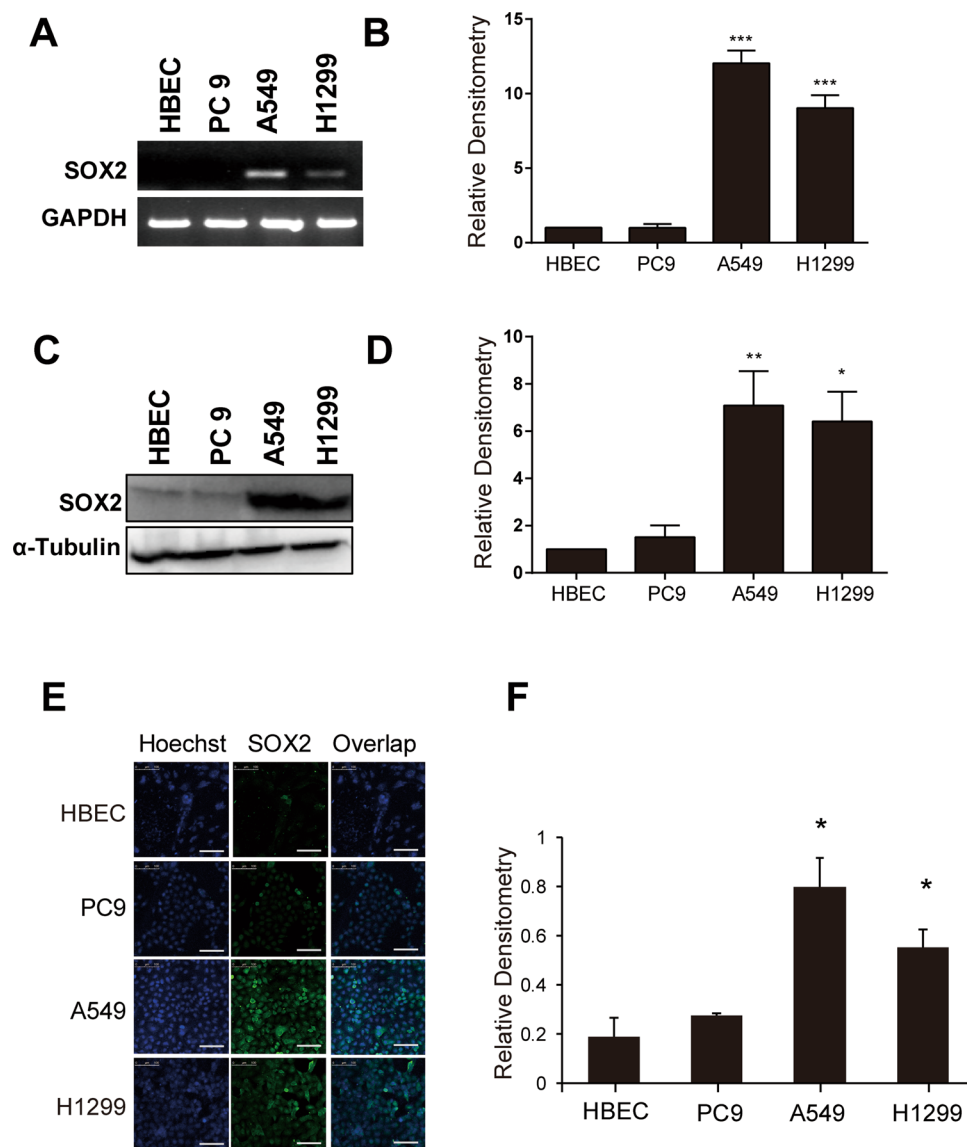
Data were analyzed with Microsoft Excel and Graphpad Prism 5 and expressed as mean  $\pm$  SD. The unpaired Student's *t* test was used to compare two groups. A *p* value < 0.05 was considered statistically significant and marked by an asterisk. A *p* value < 0.01 was marked by two asterisks. A *p* value < 0.001 was marked by three asterisks.

## Results

### SOX2 is upregulated in A549 and H1299 cells

To profile the expression of SOX2 in lung cancer cell lines, we quantitatively analyzed both mRNA and protein levels of SOX2 in three human LAD cell lines (PC9, A549 and H1299) and an immortalized normal human bronchial epithelial cell line (HBEC). As shown in Fig. 1, the assays of RT-PCR (Fig. 1a, b), immunoblotting (Fig. 1c, d) and immunofluorescent staining (Fig. 1e, f) consistently revealed that SOX2 were endogenously activated in A549 and H1299 cells compared to HBEC.

**Fig. 1** Up-regulation of SOX2 in A549 and H1299 cells. **a, b** RT-PCR analysis and quantification demonstrating that SOX2 was highly transcribed in A549 and H1299 cells compared to HBEC and PC9 cells. The housekeeping gene glyceraldehyde-3-phosphate dehydrogenase (GAPDH) was amplified as inner control. **c, d** Immunoblot analysis indicating that SOX2 was highly expressed in A549 and H1299 cells compared to HBEC and PC9 cells.  $\alpha$ -tubulin was loaded as inner control. **e, f** Immunofluorescent staining confirming aberrant high expression of SOX2 in A549 and H1299 cell nucleus. Hoechst 33342 was used to indicate cell nucleus and photos were taken under confocal laser scanning microscope. Scale bar denotes 100  $\mu$ M. Densitometry of each band was analyzed with ImageJ software. Relative densitometry was calculated by dividing grayscale of target gene with that of inner control and normalized to densitometry of HBEC. Data were analyzed by a Student's *t* test (\* $p$  < 0.05, \*\* $p$  < 0.01 and \*\*\* $p$  < 0.001 vs. HBEC)



### SS arrests growth of A549 and H1299 cells

To characterize the selective effects of selenium on LAD cells, CCK8 proliferation assay was performed to examine whether SS inhibits cell growth of HBEC, A549 and H1299 cells in time- and/or dose-dependent manners. Our data showed that SS significantly decreased the proliferation of A549 and H1299 cells and did not substantially affect HBEC cells for all time points (24, 48 and 72 h) at all three concentrations (5, 10 and 20  $\mu$ M) (Fig. 2a). Of note, cytotoxicity against HBEC cells emerged when SS was applied at 40  $\mu$ M for 48 and 72 h which justified the selective application of SS at low concentrations (5, 10 and 20  $\mu$ M) in all our following studies. Graphpad software was further applied to calculate the IC<sub>50</sub> of SS in those three above cell lines and revealed that IC<sub>50</sub> of SS in A549 and H1299 at 48 h were 23.95 and 2.82  $\mu$ M, respectively, compared to 72.9  $\mu$ M in

HBEC cells. Additional clonal formation assay showed that SS significantly repressed the clonogenicity of A549 and H1299 cells in a dose-dependent manner (Fig. 2b, c).

### SS induces and enhances programmed cell death of A549 and H1299 cells

Since SS has been reported to induce neoplastic cells of breast cancer, leukemia and colon cancer to undergo apoptosis [22, 29, 30], here we checked the efficiency of SS-mediated apoptosis induction in LAD cells. Annexin V/PI staining results showed that SS remarkably induced apoptosis in both A549 and H1299 cell lines at 10–40  $\mu$ M for 24 h. The quantitation of apoptosis cells at both early stage (lower right quadrant) and late stage (upper right quadrant) apoptotic cells in the assay of four quadrant dot plots demonstrated that SS induced the apoptosis of LAD

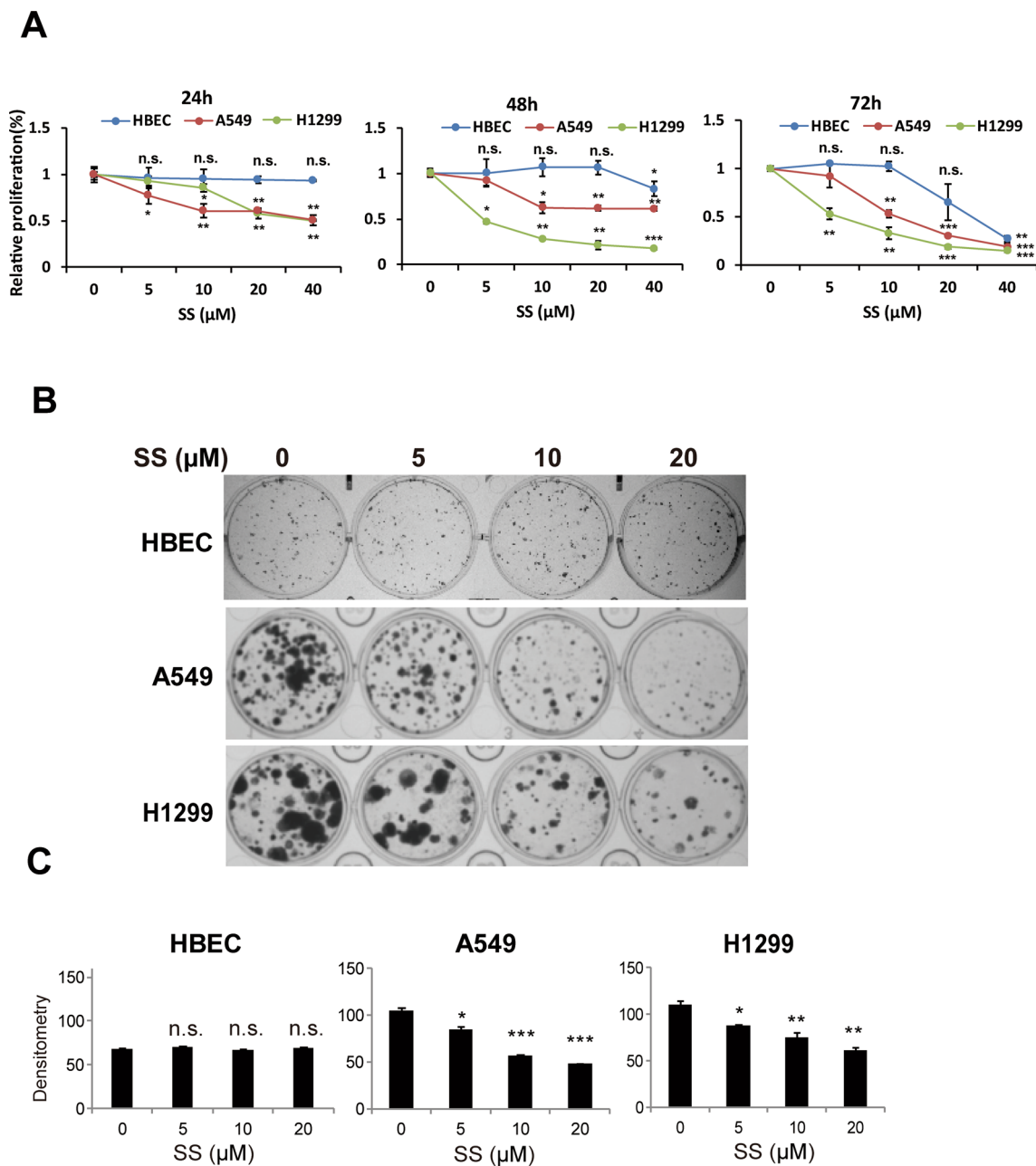


**Fig. 2** SS arrests growth of A549 and H1299 cells. **a** CCK8 assay showing that SS specifically repressed A549 and H1299 cell proliferation in a dose-dependent manner. Cells were treated with indicated concentration of SS for 24, 48 and 72 h before CCK8 test. As control (0  $\mu$ M SS), cells were incubated with same amount of PBS. The OD values for all concentrations were normalized to that of corresponding control cells and defined as relative proliferation. **b** Representa-

tive images of colony formation assay with HBEC, A549 and H1299 cells upon SS (0, 5, 10, and 20  $\mu$ M) incubation. **c** Quantification of triplicated staining of colony formation displayed that SS inhibited A549 and H1299 cell proliferative capability. Histograms are shown as mean  $\pm$  SD. Data were analyzed by a Student's *t* test (\* $p$  < 0.05, \*\* $p$  < 0.01 and \*\*\* $p$  < 0.001 vs. untreated control)

cells dose-dependently in which SS was more involved in initiation of apoptosis events (early apoptotic stage) than apoptosis progression (late apoptotic stage) in both A549 and H1299 cell lines (Fig. 3a, b).

### SS reduces the invasive growth of A549 and H1299 cells

To test whether SS additionally slows down the invasive expansion of LAD cells, we performed wound healing and

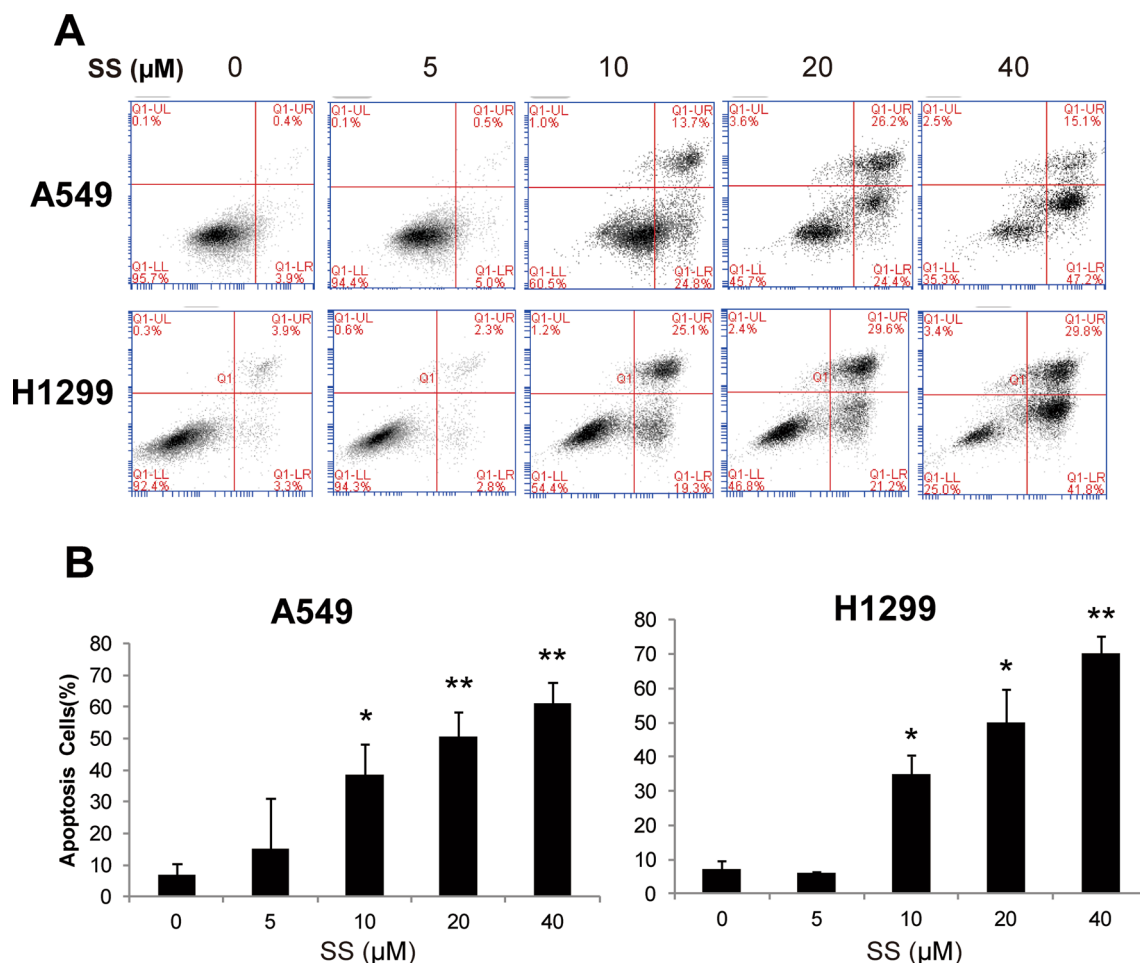


**Fig. 3** Induction of apoptosis by SS in A549 and H1299 cells. **a** Flow cytometric analysis of Annexin V/PI staining showed that SS remarkably induced apoptosis in A549 and H1299 cells. Plots were generated by Accuri C6 software package. **b** Quantification of apoptosis

ratio indicated that SS-induced apoptosis in LAD cells in a dose-dependent manner. Histograms are expressed as mean  $\pm$  SD of three independent experiments. The statistical significance was analyzed by Student's *t* test (\* $p < 0.05$ , \*\* $p < 0.01$  vs. untreated control)

transwell assay with A549 and H1299 cells upon drug incubation. Scratch healing assay showed that treatment of SS at 10  $\mu\text{M}$  for 24 h strongly blocked cell migration of both LAD cells (Fig. 4a, b), in which A549 cells was sensitive to the treatment of SS at 5  $\mu\text{M}$  for 48 h. We applied 10  $\mu\text{M}$  drug which displayed significant anti-metastatic effect in both LAD cells to further explore its role in invasion inhibition. Transwell assay further confirmed the dramatic reduction in invasive growth of A549 and H1299 cells exposed to SS at 10  $\mu\text{M}$  for 72 h (Fig. 4c).

### SS selectively targets SOX2 and its upstream hedgehog cascade signaling components to attenuate the stemness of lung cancer cells

Accumulating evidence has proven that cancer stem-like cells account for cancer initiation, progression, drug resistance and metastasis [31, 32]. The stem cell

transcription factor SOX2 and its upstream Hedgehog signaling have recently been reported to play a crucial role in the maintenance of lung cancer stemness features [33–35]. Here, we wonder if SS specifically inhibits the lung cancer stem-like cells and what are the underlying molecular mechanisms governing this event. Sphere formation assay demonstrated that SS at 10  $\mu\text{M}$  strongly reduced the number and size of A549 and H1299 cell spheroids compared to PBS control group (Fig. 5a). We next performed RT-PCR and immunoblot to examine the expression of stemness-related genes and found that treatment of SS significantly and dose-dependently down-regulated SOX2 and its upstream regulator GLI1 in A549 and H1299 cells. Of note, PTCH, a GLI1 target in Hedgehog pathway was also down-regulated, and meanwhile, another critical component of Hedgehog cascade SMO was decreased by SS only specifically for A549 not for H1299 cells (Fig. 5b, c). Consistent with immunoblotting

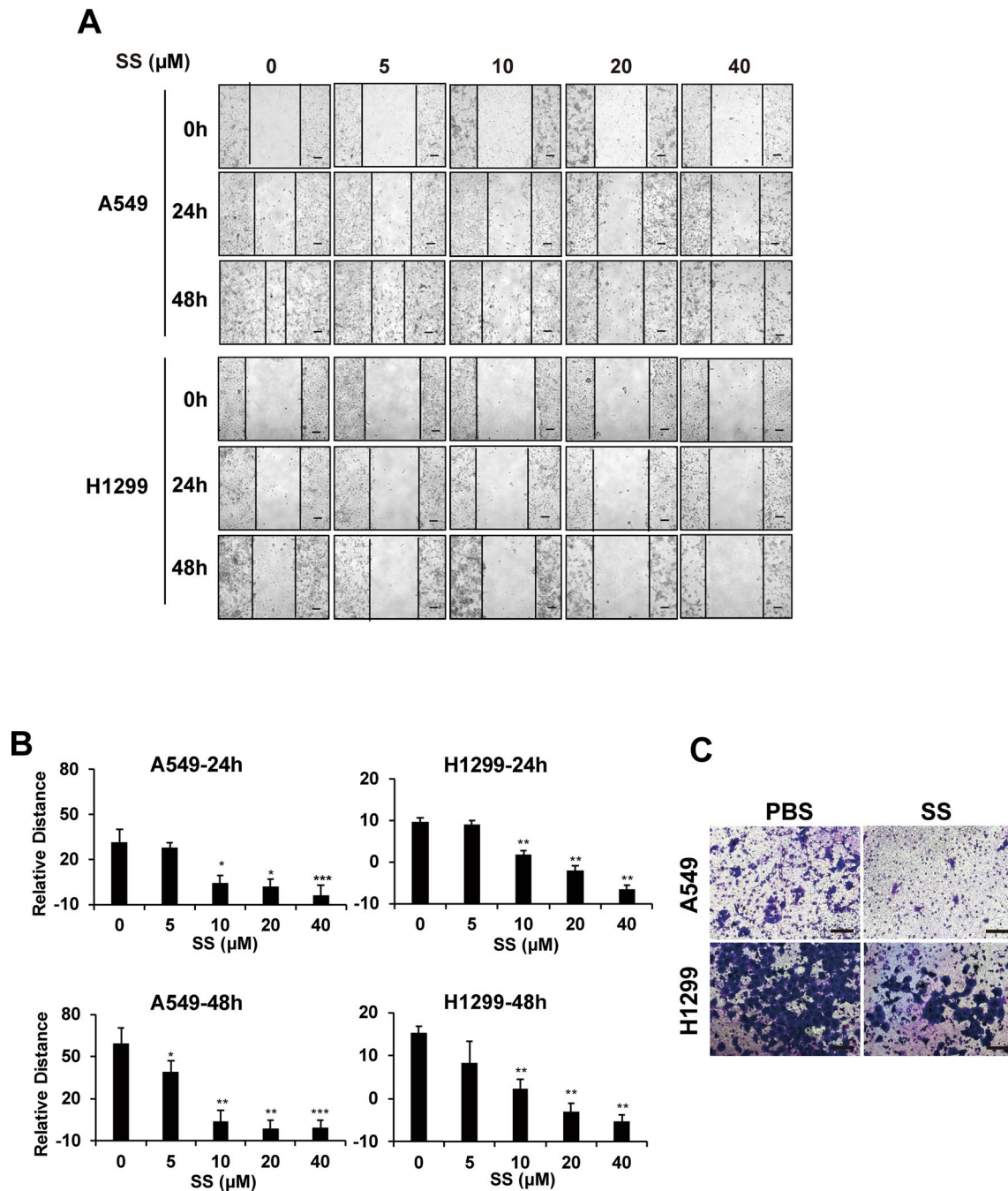


**Fig. 4** Inhibition of migration by SS in A549 and H1299 cells. **a** Wound healing assay indicated that SS repressed metastatic ability of A549 and H1299 cells after 24 and 48 h incubation. Scale bar denotes 100 μM. **b** Quantification of relative distance indicated that SS inhibited metastasis in LAD cells in a dose-dependent manner. Data were

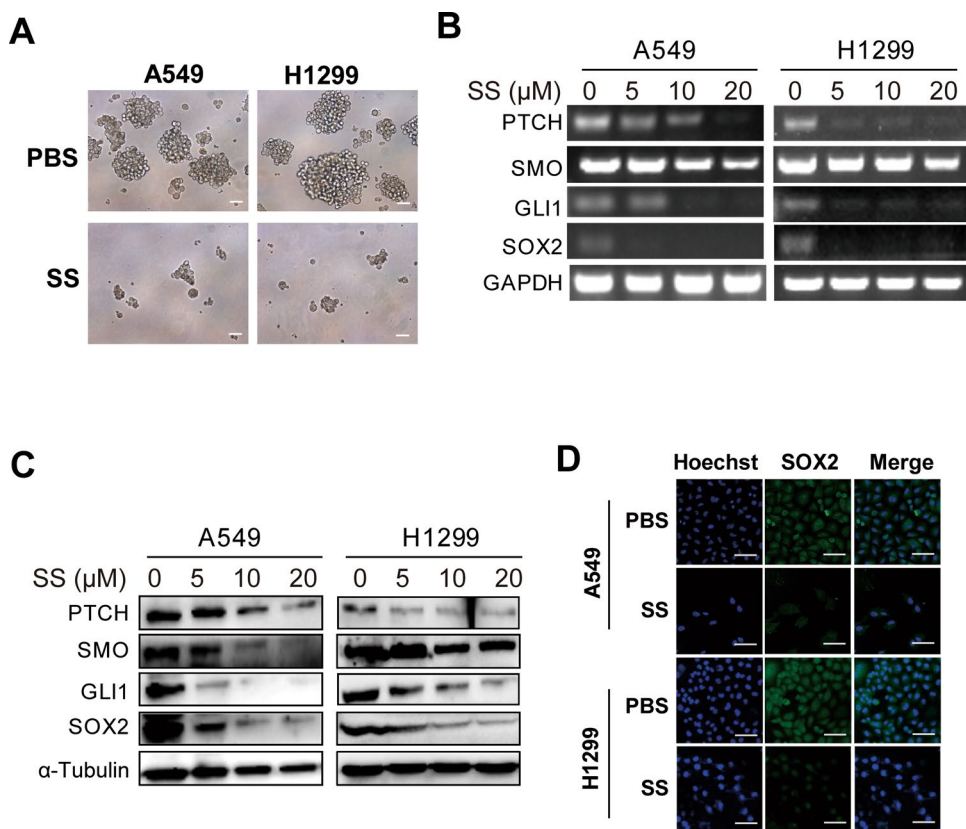
analyzed by ImageJ software. Relative distance was calculated as distance before treatment minus distance after treatment. Histograms are expressed as mean ± SD. (\*\* $p < 0.01$ , \*\*\* $p < 0.001$  vs. untreated control). **c** Transwell assay demonstrated that SS prohibited invasive capability of A549 and H1299 cells. Scale bar denotes 50 μM

result, immunofluorescent staining indicated that SS treatment decreased SOX2 expression level in nucleus of A549 and H1299 (Fig. 5d).

### The pivotal role of SOX2 in SS-mediated cancer growth inhibition

To specify and manifest the phenotypic function of SOX2, A549 and H1299 cells were transfected with pcDNA 3.1

**Fig. 5** SS selectively targets SOX2–SHH signal circuitry in lung cancer cells. **a** SS retarded sphere forming capability of A549 and H1299 cells. Scale bar denotes 50  $\mu$ M. **b** RT-PCR analysis demonstrating that SS decreased transcriptional levels of SOX2 and Hedgehog cascade components (PTCH, SMO and GLI1) in A549 and H1299 cells. **c** Immunoblot analysis demonstrating that SS reduced protein level of SOX2 and Hedgehog cascade components (PTCH, SMO and GLI1) in A549 and H1299 cells. **d** Immunofluorescent staining showed that SS at 10  $\mu$ M significantly decreased nucleus SOX2 expression in A549 and H1299 cells compared to PBS incubated control samples. Scale bar denotes 50  $\mu$ M



based SOX2 plasmid (SOX2) to gain the forced expression of SOX2 and empty vector pcDNA 3.1 (pc3.1) as control. As indicated in Fig. 6a, b, SOX2 overexpression was verified in A549 and H1299 cells with assays of both RT-PCR and immunofluorescent staining. CCK8 assay showed that SOX2 overexpression significantly arrested SS-mediated A549 growth inhibition at all selected concentrations (5, 10, 20 and 40  $\mu$ M) while those phenomena were not observed in H1299 cells except at 20  $\mu$ M SS treatment with relative mild effects which suggests that more alternative targets of SS may exist in addition to SOX2 (Fig. 6c). Clonal formation assay revealed that forced expression of SOX2 enhanced clonogenicity of A549 and H1299 cells and significantly resisted SS-induced reduction in clonal expansion ability of those LAD cells in dose-dependent manner (Fig. 6d, e).

## Discussion

In the present study, we found that SS exhibited remarkable anti-proliferative and pro-apoptotic ability in SOX2 positive LAD cell lines in a dose-dependent manner with no or marginal effect on normal lung epithelial cells. SOX2, as a stem cell transcription factor, was previously reported to be highly expressed in lung squamous carcinoma cells [36]. Here we identified two LAD cell lines A549 and H1299 harboring

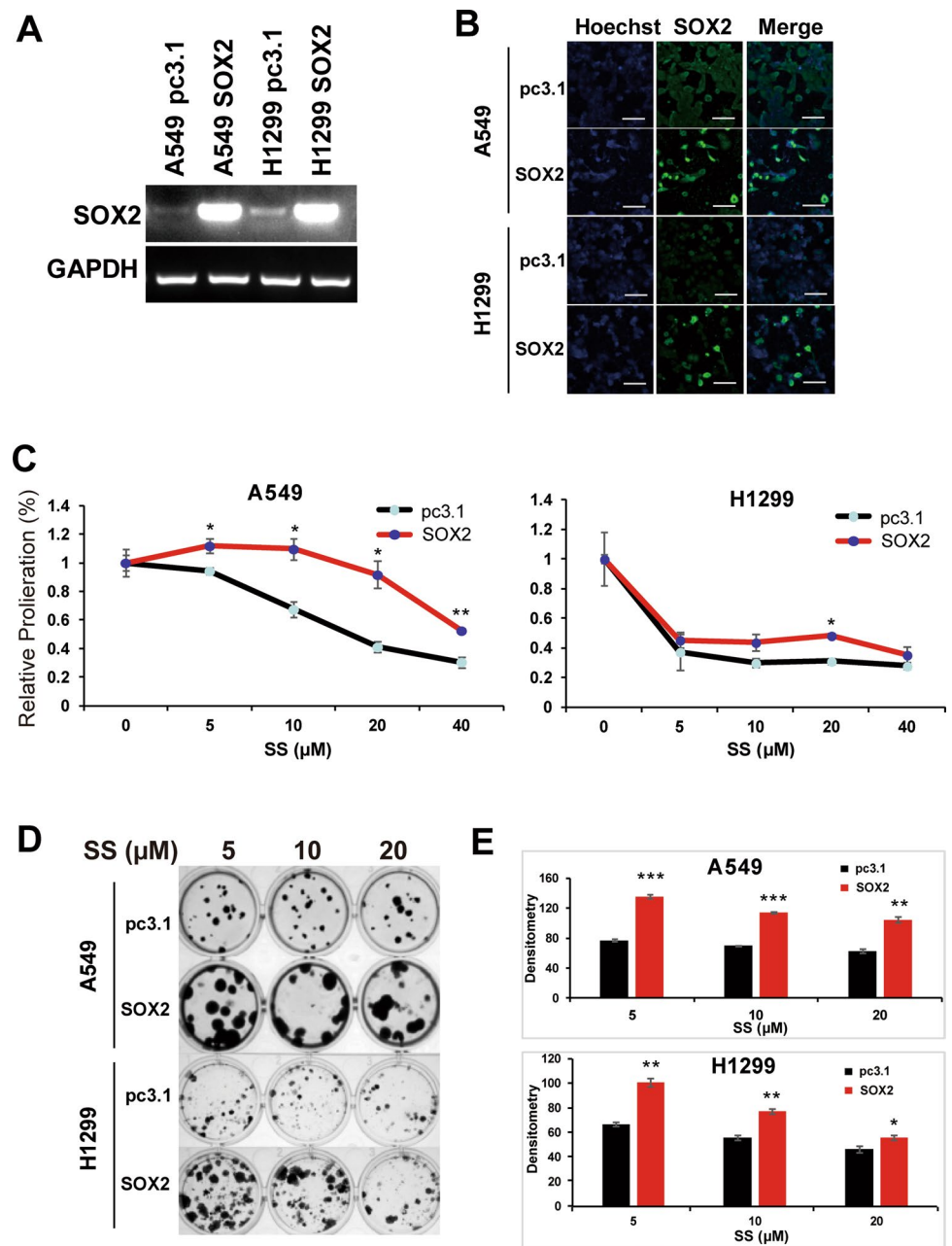
aberrant high SOX2 expression compared with normal human epithelial cell line HBEC. Our in vitro assays further demonstrated that SS attenuated lung adenocarcinoma progression by repressing SOX2 and its upstream regulator GLI1, which suggests that SS may be a potential therapeutic drug candidate for lung cancer patients.

SS has been reported to be able to disrupt disease progression in 38% of patients with reversible and bearable side effects when administered up to 10.2 mg/m<sup>2</sup> in a phase I clinical trial including 70% lung carcinoma patients who were resistant to cytostatic drugs [16]. When those patients were administered with SS at 10.2 mg/m<sup>2</sup>/day for 2 weeks, the plasma selenium concentration ranged from 5 to 25  $\mu$ M [16], which might justify the drug concentrations (5–20  $\mu$ M) employed in our settings to test anti-proliferative and pro-apoptotic efficiency. While Karp et al. [37] announced a negative relevance between selenized yeast uptake and clinical benefits in a phase I clinical trial for NSCLC, we reasoned that application and formula of SS might matter in explaining the different outcomes of those clinical trials.

Previous studies reported that downregulation of SOX2 expression in lung cancer stem cells effectively inhibited tumorigenicity, drug resistance and metastasis in vitro and in vivo [35, 38, 39]. Our data showed that SS at 10  $\mu$ M abrogated stemness sphere formation of LAD cells in vitro and reduced SOX2 expression. Furthermore, forced expression



**Fig. 6** SOX2 overexpression counteracted anti-proliferative capability of SS in LAD cells. **a** RT-PCR analysis demonstrating exogenous SOX2 transcription in A549 and H1299 cells. **b** Immunofluorescent staining showing SOX2 overexpression in A549 and H1299 cells compared to respective pc3.1 transfected cells. Scale bar denotes 50  $\mu$ M. **c** CCK8 assay revealed that SOX2 overexpression neutralized anti-proliferative capability of SS in LAD cells. **d, e** Clonal formation assay and quantification displayed that SOX2 transfected cells were more resistant to SS treatment. Histograms are expressed as mean  $\pm$  SD of three independent experiments. The statistical significance was analyzed by Student's *t* test (\* $p < 0.05$ , \*\* $p < 0.01$ , \*\*\* $p < 0.001$  vs. respective concentration of drug incubated cells)



of SOX2 counteracted the anti-proliferative capacity of SS as shown in our CCK8 and clonal formation assays. Our findings confirmed that SS targets pluripotency of lung cancer cells via selectively repressing SOX2. Previous studies have proven that drug-resistant lung cancer cells were sensitive to SS incubation when used at high concentrations (100–500  $\mu$ M) for short term (6 h) or relative low concentration (5–30  $\mu$ M) for up to 5 days [40, 41]. Since cancer stem-like cells play essential roles in drug resistance formation, SS could re-sensitize lung cancer cells with drug resistance by targeting cancer stem-like cells.

As a positive upstream regulator of SOX2, GLI1 has been identified to be related to lung cancer progression,

drug resistance formation and stem-related feature maintenance [7, 13]. Our previous findings showed that GLI1 was highly upregulated in lung cancer tissues compared with their paired normal adjacent tissues [11]. Disruption of Hedgehog cascade was proved to prohibit proliferation of NSCLC cells and sensitize NSCLC cells to cisplatin therapy in vivo [11]. Thus, we further explored whether SS down-regulated SOX2 via modulating its upstream regulator GLI1. Our data indicated that SS repressed GLI1 consistently and targeted other Hedgehog cascade molecules selectively in LAD cells which suggested that SS mediated specific inhibition of GLI1–SOX2 axis in those lung cancer cells.

The mechanisms governing the SS-mediated growth inhibition of lung cancer stem cells are complex and SS may have multiple targets in addition to GLI1–SOX2 axis. Although we have briefly explored SS's antitumor effect in vitro, how SS worked in vivo to retard tumor initiation, progression and metastasis remains to be addressed in our future study. In summary, our study demonstrated that SS inhibited LAD cell proliferation and stemness traits through targeting SOX2 and its upstream factor GLI1. This provides experimental evidence that SS could eradicate cancer stem-like cells in vitro and might potentially facilitate LAD therapy in clinic.

**Funding** This study was supported by Foundation for Outstanding Young Scientist of Natural Science Foundation of Shandong Province (BS2014YY016), Binzhou Science and Technology grant (2015ZCO333), Yantai Science and Technology Grant (2015ZH080), Binzhou Medical College Grant (BY2015KJ02, BY2015KYQD28), Projects of Medical and Health Technology Development Program of Shandong Province (2017WS155) and Foundation for General Project of Natural Science Foundation of Shandong Province (ZR2016HM57).

## Compliance with ethical standards

**Conflict of interest** All authors declare that they have no conflict of interest.

**Ethical approval** This article does not contain any studies with human participants or animals performed by any of the authors.

## References

- Chen Z, Fillmore CM, Hammerman PS, Kim CF, Wong KK (2014) Non-small-cell lung cancers: a heterogeneous set of diseases. *Nat Rev Cancer* 14(8):535–546. <https://doi.org/10.1038/nrc3775>
- Siegel RL, Miller KD, Jemal A (2016) Cancer statistics, 2016. *CA Cancer J Clin* 66(1):7–30. <https://doi.org/10.3322/caac.21332>
- Reck M, Heigener DF, Mok T, Soria J-C, Rabe KF (2013) Management of non-small-cell lung cancer: recent developments. *The Lancet* 382(9893):709–719. [https://doi.org/10.1016/s0140-6736\(13\)61502-0](https://doi.org/10.1016/s0140-6736(13)61502-0)
- Chong CR, Janne PA (2013) The quest to overcome resistance to EGFR-targeted therapies in cancer. *Nat Med* 19(11):1389–1400. <https://doi.org/10.1038/nm.3388>
- Adorno-Cruz V, Kibria G, Liu X, Doherty M, Junk DJ, Guan D, Hubert C, Venere M, Mulkearns-Hubert E, Sinyuk M, Alvarado A, Caplan AI, Rich J, Gerson SL, Lathia J, Liu H (2015) Cancer stem cells: targeting the roots of cancer, seeds of metastasis, and sources of therapy resistance. *Cancer Res* 75(6):924–929. <https://doi.org/10.1158/0008-5472.can-14-3225>
- Sourisseau T, Hassan KA, Wistuba I, Penault-Llorca F, Adam J, Deutsch E, Soria JC (2014) Lung cancer stem cell: fancy conceptual model of tumor biology or cornerstone of a forthcoming therapeutic breakthrough? *J Thorac Oncol* 9(1):7–17. <https://doi.org/10.1097/JTO.000000000000028>
- Bora-Singhal N, Perumal D, Nguyen J, Chellappan S (2015) Gli1-mediated regulation of Sox2 facilitates self-renewal of stem-like cells and confers resistance to EGFR inhibitors in non-small cell lung cancer. *Neoplasia* 17(7):538–551. <https://doi.org/10.1016/j.neo.2015.07.001>
- Takebe N, Miele L, Harris PJ, Jeong W, Bando H, Kahn M, Yang SX, Ivy SP (2015) Targeting Notch, Hedgehog, and Wnt pathways in cancer stem cells: clinical update. *Nat Rev Clin Oncol* 12(8):445–464. <https://doi.org/10.1038/nrclinonc.2015.61>
- Amakye D, Jagani Z, Dorsch M (2013) Unraveling the therapeutic potential of the Hedgehog pathway in cancer. *Nat Med* 19(11):1410–1422. <https://doi.org/10.1038/nm.3389>
- Leem YE, Ha HL, Bae JH, Baek KH, Kang JS (2014) CDO, an Hh-coreceptor, mediates lung cancer cell proliferation and tumorigenicity through Hedgehog signaling. *PLoS one* 9(11):e111701. <https://doi.org/10.1371/journal.pone.0111701>
- Du J, Chen W, Yang L, Dai J, Guo J, Wu Y, Gong K, Zhang J, Yu N, Xie Z, Xi S (2017) Disruption of SHH signaling cascade by SBE attenuates lung cancer progression and sensitizes DDP treatment. *Sci Rep* 7(1):1899. <https://doi.org/10.1038/s41598-017-02063-x>
- Della Corte CM, Bellecine C, Vicidomini G, Vitagliano D, Malapelle U, Accardo M, Fabozzi A, Fiorelli A, Fasano M, Papaccio F, Martinelli E, Troiani T, Troncone G, Santini M, Bianco R, Ciardiello F, Morgillo F (2015) SMO gene amplification and activation of the hedgehog pathway as novel mechanisms of resistance to anti-epidermal growth factor receptor drugs in human lung cancer. *Clin Cancer Res* 21(20):4686–4697. <https://doi.org/10.1158/1078-0432.ccr-14-3319>
- Ahmad A, Maitah MY, Ginnebaugh KR, Li Y, Bao B, Gadjeel SM, Sarkar FH (2013) Inhibition of Hedgehog signaling sensitizes NSCLC cells to standard therapies through modulation of EMT-regulating miRNAs. *J Hematol Oncol* 6(1):77. <https://doi.org/10.1186/1756-8722-6-77>
- Wrobel JK, Power R, Toborek M (2016) Biological activity of selenium: revisited. *IUBMB life* 68(2):97–105. <https://doi.org/10.1002/iub.1466>
- Fernandes AP, Gandin V (2015) Selenium compounds as therapeutic agents in cancer. *Biochim Biophys Acta* 1850(8):1642–1660. <https://doi.org/10.1016/j.bbagen.2014.10.008>
- Brodin O, Eksborg S, Wallenberg M, Asker-Hagelberg C, Larsen EH, Mohlkert D, Lenneby-Helleday C, Jacobsson H, Linder S, Misra S, Bjornstedt M (2015) Pharmacokinetics and toxicity of sodium selenite in the treatment of patients with carcinoma in a phase I clinical trial: The SECAR Study. *Nutrients* 7(6):4978–4994. <https://doi.org/10.3390/nu7064978>
- Okuno T, Honda E, Arakawa T, Ogino H, Ueno H (2014) Glutathione-dependent cell cycle G1 arrest and apoptosis induction in human lung cancer A549 cells caused by methylseleninic acid: comparison with sodium selenite. *Biol Pharm Bull* 37(11):1831–1837. <https://doi.org/10.1248/bpb.b14-00453>
- Shigemitsu Z, Manabe K, Hara N, Baba Y, Hosokawa K, Kagawa H, Watanabe T, Fujimuro M (2017) Methylseleninic acid and sodium selenite induce severe ER stress and subsequent apoptosis through UPR activation in PEL cells. *Chem Biol Interact* 266:28–37. <https://doi.org/10.1016/j.cbi.2017.01.027>
- Shi K, Jiang Q, Li Z, Shan L, Li F, An J, Yang Y, Xu C (2013) Sodium selenite alters microtubule assembly and induces apoptosis in vitro and in vivo. *J Hematol Oncol* 6:7. <https://doi.org/10.1186/1756-8722-6-7>
- Li Z, Meng J, Xu TJ, Qin XY, Zhou XD (2013) Sodium selenite induces apoptosis in colon cancer cells via Bax-dependent mitochondrial pathway. *Eur Rev Med Pharmacol Sci* 17(16):2166–2171
- Chen P, Wang L, Li N, Liu Q, Ni J (2013) Comparative proteomics analysis of sodium selenite-induced apoptosis in human prostate cancer cells. *Metallomics* 5(5):541–550. <https://doi.org/10.1039/c3mt00002h>

22. Kralova V, Benesova S, Cervinka M, Rudolf E (2012) Selenite-induced apoptosis and autophagy in colon cancer cells. *Toxicol In Vitro* 26(2):258–268. <https://doi.org/10.1016/j.tiv.2011.12.010>
23. Fu L, Liu Q, Shen L, Wang Y (2011) Proteomic study on sodium selenite-induced apoptosis of human cervical cancer HeLa cells. *J Trace Elements Med Biol* 25(3):130–137. <https://doi.org/10.1016/j.jtemb.2011.06.001>
24. Freitas M, Alves V, Sarmento-Ribeiro AB, Mota-Pinto A (2011) Combined effect of sodium selenite and docetaxel on PC3 metastatic prostate cancer cell line. *Biochem Biophys Res Commun* 408(4):713–719. <https://doi.org/10.1016/j.bbrc.2011.04.109>
25. Berggren M, Sittadjody S, Song Z, Samira JL, Burd R, Meuillet EJ (2009) Sodium selenite increases the activity of the tumor suppressor protein, PTEN, in DU-145 prostate cancer cells. *Nutr Cancer* 61(3):322–331. <https://doi.org/10.1080/01635580802521338>
26. Tian J, Ning S, Knox SJ (2010) Sodium selenite radiosensitizes hormone-refractory prostate cancer xenograft tumors but not intestinal crypt cells in vivo. *Int J Radiat Oncol Biol Phys* 78(1):230–236. <https://doi.org/10.1016/j.ijrobp.2010.03.006>
27. Pfister C, Dawczynski H, Schingale FJ (2016) Sodium selenite and cancer related lymphedema: biological and pharmacological effects. *J Trace Elements Med Biol* 37:111–116. <https://doi.org/10.1016/j.jtemb.2016.05.005>
28. Du J, Neuenschwander M, Yu Y, Dabritz JH, Neuendorff NR, Schleich K, Bittner A, Milanovic M, Beuster G, Radetzki S, Specker E, Reimann M, Rosenbauer F, Mathas S, Lohneis P, Hummel M, Dorken B, von Kries JP, Lee S, Schmitt CA (2017) Pharmacological restoration and therapeutic targeting of the B-cell phenotype in classical Hodgkin lymphoma. *Blood* 129(1):71–81. <https://doi.org/10.1182/blood-2016-02-700773>
29. Zhang W, Xiao H, Parkin KL (2014) Apoptosis in MCF-7 breast cancer cells induced by S-alkenylmercaptocysteine (CySSR) species derived from Allium tissues in combination with sodium selenite. *Food Chem Toxicol* 68:1–10. <https://doi.org/10.1016/j.fct.2014.03.002>
30. Cao TM, Hua FY, Xu CM, Han BS, Dong H, Zuo L, Wang X, Yang Y, Pan HZ, Zhang ZN (2006) Distinct effects of different concentrations of sodium selenite on apoptosis, cell cycle, and gene expression profile in acute promyelocytic leukemia-derived NB4 cells. *Ann Hematol* 85(7):434–442. <https://doi.org/10.1007/s00277-005-0046-4>
31. Zhao C, Chen A, Jamieson CH, Fereshteh M, Abrahamsson A, Blum J, Kwon HY, Kim J, Chute JP, Rizzieri D, Munchhof M, VanArsdale T, Beachy PA, Reya T (2009) Hedgehog signalling is essential for maintenance of cancer stem cells in myeloid leukaemia. *Nature* 458(7239):776–779. <https://doi.org/10.1038/nature07737>
32. Cai J, Fang L, Huang Y, Li R, Xu X, Hu Z, Zhang L, Yang Y, Zhu X, Zhang H, Wu J, Huang Y, Li J, Zeng M, Song E, He Y, Zhang L, Li M (2017) Simultaneous overactivation of Wnt/beta-catenin and TGFbeta signalling by miR-128-3p confers chemoresistance-associated metastasis in NSCLC. *Nat Commun* 8:15870. <https://doi.org/10.1038/ncomms15870>
33. Po A, Silvano M, Miele E, Capalbo C, Eramo A, Salvati V, Todaro M, Besharat ZM, Catanzaro G, Cucchi D, Coni S, Di Marcotullio L, Canettieri G, Vacca A, Stassi G, De Smaele E, Tartaglia M, Screpanti I, De Maria R, Ferretti E (2017) Noncanonical GLI1 signaling promotes stemness features and in vivo growth in lung adenocarcinoma. *Oncogene*. <https://doi.org/10.1038/nc.2017.91>
34. Xia Y, Wu Y, Liu B, Wang P, Chen Y (2014) Downregulation of miR-638 promotes invasion and proliferation by regulating SOX2 and induces EMT in NSCLC. *FEBS Lett* 588(14):2238–2245. <https://doi.org/10.1016/j.febslet.2014.05.002>
35. Chou YT, Lee CC, Hsiao SH, Lin SE, Lin SC, Chung CH, Chung CH, Kao YR, Wang YH, Chen CT, Wei YH, Wu CW (2013) The emerging role of SOX2 in cell proliferation and survival and its crosstalk with oncogenic signaling in lung cancer. *Stem cells* 31(12):2607–2619. <https://doi.org/10.1002/stem.1518>
36. Lu Y, Futtner C, Rock JR, Xu X, Whitworth W, Hogan BL, Onaitis MW (2010) Evidence that SOX2 overexpression is oncogenic in the lung. *PloS one* 5(6):e11022. <https://doi.org/10.1371/journal.pone.0011022>
37. Karp DD, Lee SJ, Keller SM, Wright GS, Aisner S, Belinsky SA, Johnson DH, Johnston MR, Goodman G, Clamon G, Okawara G, Marks R, Frechette E, McCaskill-Stevens W, Lippman SM, Ruckdeschel J, Khuri FR (2013) Randomized, double-blind, placebo-controlled, phase III chemoprevention trial of selenium supplementation in patients with resected stage I non-small-cell lung cancer: ECOG 5597. *J Clin Oncol* 31(33):4179–4187. <https://doi.org/10.1200/jco.2013.49.2173>
38. Xiang R, Liao D, Cheng T, Zhou H, Shi Q, Chuang TS, Markowitz D, Reisfeld RA, Luo Y (2011) Downregulation of transcription factor SOX2 in cancer stem cells suppresses growth and metastasis of lung cancer. *Br J Cancer* 104(9):1410–1417. <https://doi.org/10.1038/bjc.2011.94>
39. Chen S, Xu Y, Chen Y, Li X, Mou W, Wang L, Liu Y, Reisfeld RA, Xiang R, Lv D, Li N (2012) SOX2 gene regulates the transcriptional network of oncogenes and affects tumorigenesis of human lung cancer cells. *PloS one* 7(5):e36326. <https://doi.org/10.1371/journal.pone.0036326>
40. Caffrey PBF. (1994) The development of drug resistance by tumor cells in vitro is accompanied by the development of sensitivity to selenite. *Cancer Lett* 81(1):59–65
41. Bjorkhem-Bergman L, Jonsson K, Eriksson LC, Olsson JM, Lehmann S, Paul C, Bjornstedt M (2002) Drug-resistant human lung cancer cells are more sensitive to selenium cytotoxicity. Effects on thioredoxin reductase and glutathione reductase. *Biochem Pharmacol* 63(10):1875–1884